

See discussions, stats, and author profiles for this publication at: <https://www.researchgate.net/publication/231645738>

Photoluminescence Lifetime of Lead Selenide Colloidal Quantum Dots

ARTICLE *in* THE JOURNAL OF PHYSICAL CHEMISTRY C · AUGUST 2010

Impact Factor: 4.77 · DOI: 10.1021/jp105818e

CITATIONS

27

READS

29

2 AUTHORS:



Heng Liu

University of Chicago

12 PUBLICATIONS 142 CITATIONS

SEE PROFILE



guyot-sionnest Philippe

University of Chicago

174 PUBLICATIONS 12,326 CITATIONS

SEE PROFILE

Photoluminescence Lifetime of Lead Selenide Colloidal Quantum Dots

Heng Liu and Philippe Guyot-Sionnest*

James Franck Institute, The University of Chicago, 929 East 57th Street, Chicago, Illinois 60637

Received: June 23, 2010; Revised Manuscript Received: August 4, 2010

The photoluminescence (PL) lifetime of PbSe colloidal quantum dots (QDs) is investigated. At room temperature, the surface ligands have a dominant effect on the PL lifetime of PbSe nanocrystals emitting photon with energy between 0.55 and 0.72 eV. Above 0.75 eV, the decay rate follows approximately a linear relationship with PL energy. At low temperature, the lifetime increases from 200 ns to nearly 1 μ s, but the PL efficiency does not increase significantly. The model of dipole energy transfer to the ligands vibrations accounts rather well for the observations.

I. Introduction

Compared with organic materials, colloidal semiconductor nanocrystals made with materials of low phonon frequency have potential for infrared materials. Quantum dots (QDs) made from narrow gap PbSe exhibit a well-defined excitonic structure and have near-unity quantum yield with emission wavelength in the near-infrared regime (below 1.6 μ m).^{1,2} However, the PL efficiency of the PbSe dots decreases strongly as the size increases.³ A dipole energy transfer model was introduced to account quantitatively for energy transfer of mid-IR electronic excitation to the vibrations of the ligands.⁴ Here we investigate the energy relaxation of PbSe colloidal samples and show that the decay rate can, to a large extent, be explained by the dipole energy transfer model.

II. Experimental Details

Materials and Synthesis. The samples in this study are of two types. One is PbSe nanocrystal, which is used for fluorescence and lifetime measurement over different PL energies as well as low temperature measurement. The other is a PbSe/CdSe core/shell, which is mainly used for the ligand replacement. The PbSe colloidal QDs are prepared following ref 5, and the PbSe/CdSe core/shell is prepared following ref 6.

PbSe Nanocrystals. Lead acetate (0.54 g, 1.66 M) was dissolved in 1.8 mL of oleic acid and 10 mL of 1-octadecene (ODE). The solution was heated to 100 °C in vacuum for \sim 2 h to form lead oleate. Then, the temperature was increased to 180 °C under argon. TOP Se (4.5 mL, 1 M) was injected into the solution as soon as the temperature reached 180 °C. The reaction time varied from 5 s to 1 min to obtain PbSe with the desired sizes. The solution was cooled by the addition of 5 mL of toluene and 5 mL of hexane.

CdSe Shell. CdO (0.25 g), 1.5 mL of oleic acid, and 3.7 mL of ODE were heated to 100 °C in vacuum to remove water and oxygen, then to 255 °C under argon for 1 h to form cadmium oleate (CdOA). After all CdO had dissolved, the solution was cooled to 120 °C. Separately, 10 mL of liquid from the PbSe solution was cleaned once by ethanol and centrifuged. The PbSe solid was dissolved in 2 mL of toluene and degassed by Ar at room temperature for more than 1 h. The temperature was

increased to 100 °C rapidly, and the CdOA solution previously prepared was immediately injected. The solution was stirred under Ar flow at 100 °C for more than 1 h.

Ligand Replacement. A 2 mL sample solution after CdOA treatment (\sim 10 μ mol PbSe) was cleaned once with ethanol and dispersed in chloroform. The ligand, perfluorotetradecanoic acid (15 mg, \sim 20 μ mol), was dissolved in 1 mL of perfluoro-1,3-dimethylcyclohexane and then heated to about 70–80 °C to increase the solubility of the acid, followed by immediate mixing of the QD and ligand solution. After a few seconds of shaking and stirring, nearly all QDs leave the chloroform layer for the perfluoro-1,3-dimethylcyclohexane layer.

Experimental Setup. All absorption spectra were taken with a Fourier transform infrared spectrometer (Thermo Nexus 670 FT IR) operating from 2000 to 11000 cm^{-1} or from 400 to 7000 cm^{-1} . We utilized a Nd/YAG laser system operating at 25 Hz providing picosecond laser pulses at 1064 nm wavelength. For all of the room-temperature measurement, the sample was dissolved in tetrachloroethylene (TCE) and placed in a 1 mm thick glass cell. The fluorescence was collected by a paraboloidal mirror and sent to a flat grating with 600 grooves per millimeter. Another paraboloidal mirror was used to focus the diffracted light onto a HgCdTe infrared detector (Kolmar KMPV 1-1-J1/DC). A 1064 nm laser mirror was used in front of the detector to reduce the scattered 1064 nm light from the sample. Lifetime measurements were taken with a digital oscilloscope (Tektronix TDS1012B). For the low-temperature spectroscopy, instead of TCE, 2,2,4,4,6,6,8,8-heptamethylnonane, a low-temperature glass former, was the solvent for PbSe nanocrystal, and the cell was made of two sapphire windows with 0.75 mm spacing. The sample was cooled in a closed cycle cryostat.

III. Results and Discussion

Figure 1 shows the normalized PL intensity with different PL energies from 0.55 to 0.85 eV. It indicates that the smaller dots give higher signal. As shown in Figure 2, the lifetimes are longer for the smaller nanocrystals and shorter for the larger nanocrystals, which are at lower energy. This trend is in contradiction with the expected behavior of the radiative rates but in agreement with the reduced PL efficiency for larger nanocrystals.³

From Fermi's golden rule, the radiative rate of a transition dipole including screening¹ is (in CGS unit)

* To whom correspondence should be addressed. E-mail: pgs@uchicago.edu.

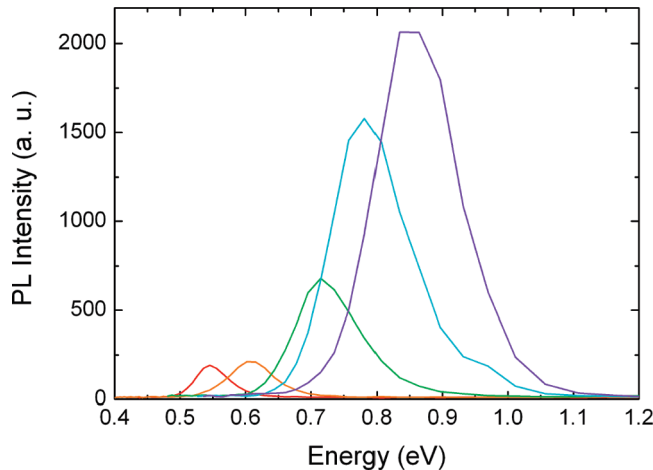


Figure 1. PL of PbSe of various sizes at room temperature. (The PL intensity is normalized by the absorbance at the excitation wavelength of 1064 nm.)

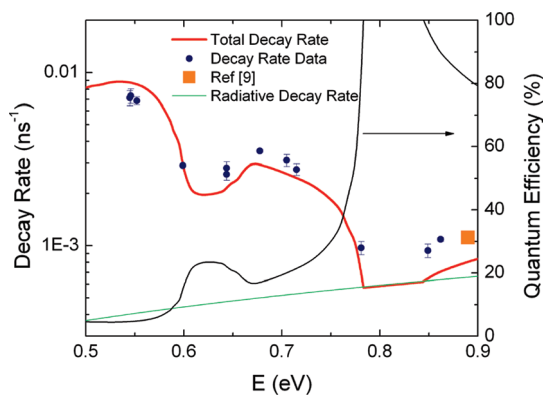


Figure 2. Decay rates of PbSe of various sizes at room temperature. Blue dots are from the lifetime measurement. The solid red line is the total decay rate, $T^{-1} = T_{nr}^{-1} + T_r^{-1}$, based on eqs 1 and 5 with no adjustable parameter. The green line is the radiative rate calculated with no adjustable parameter using eq 1. The theoretical result of An et al.¹¹ is shown as an orange square. The black curve shows the quantum efficiency based on T_r^{-1}/T^{-1} .

$$T_r^{-1} = \left(\frac{3\epsilon_m}{\epsilon_1 + 2\epsilon_2} \right)^2 \frac{4e^2 \sqrt{\epsilon_m} \omega P^2}{3m_0^2 c^3 \hbar} \quad (1)$$

where ω is the photon frequency, e is the electron charge, m_0 is the free mass of the electron, c is the speed of light, \hbar is the reduced Planck constant, and ϵ_m and ϵ_1 are the dielectric constant of solvent and PbSe, respectively. P is the Kane interband parameter, which does not depend on the size of the nanocrystals. In eq 1, the oscillator strength of the emitting state and the dielectric constants are taken to be size-independent. We note that in the size range considered here (5–8 nm), experimental values for the oscillator strength do not indicate a clear variation but that a linear trend has been proposed based on theory.^{7,8} Measurement and theory for the size range considered also indicate that the variations of the dielectric constant should be smaller than $\sim 20\%$.⁹ Such effects might lead to small corrections over the order of magnitude trend that we attempt to explain. Taking $2P^2/m_0 = 3$ eV,¹⁰ $\epsilon_m = 2.25$ for TCE, and $\epsilon_1 = 23$ for PbSe, the radiative decay rate is $T_r^{-1} = 3.9 \times 10^{-3} \text{ ns}^{-1} \text{ eV}^{-1} \times \text{energy (eV)}$.

An et al.¹¹ calculated the lifetimes using an atomistic pseudopotential and provided a theoretical value of 897 ns for 0.89 eV (point shown in Figure 2). Equation 1 neglects the

degeneracy of the exciton and overestimates the decay rate. There are 64 excitons arising from the four equivalent gaps at the L-points in Brillouin zone.¹² Neglecting spin–orbit, there is one bright singlet state and three dark triplet states in each valley.¹³ Introducing the rather strong spin–orbit coupling,¹¹ the total angular momentum of conduction and valence band states gives instead three bright states and one dark state per valley.¹¹ Assuming that the intervalley transitions are forbidden, this yields 12 bright states. Therefore, we multiply eq 1 by a degeneracy factor of 12/64 when calculating the decay rate. The result is shown as a green line in Figure 2 and slightly underestimates the decay rate compared with the pseudopotential result.

There are many possible models to describe nonradiative process. In the infrared energy range, where the molecular vibration occurs, the rate could be strongly affected with ligand vibrations. In a simple model,^{4,14} the electronic transition in the spherical nanocrystal transfers its energy to a shell of molecular vibrational modes by dipole coupling. Assuming that the PbSe nanocrystal (radius R) is surrounded by a uniform ligand shell with imaginary dielectric constant ϵ'' and thickness ΔR , the nonradiative rate is expressed as (in CGS units)

$$T_{nr}^{-1} = \left(\frac{3\epsilon_m}{\epsilon_1 + 2\epsilon_2} \right)^2 \epsilon'' \frac{p_0^2}{\hbar} \int_R^{R+\Delta R} \frac{dR}{R^4} = \left(\frac{3\epsilon_m}{\epsilon_1 + 2\epsilon_2} \right)^2 \epsilon'' \frac{4\pi p_0^2}{9\hbar} \times \left(\frac{1}{V_1} - \frac{1}{V_2} \right) \quad (2)$$

where p_0 is the dipole transition moment and $p_0^2 = e^2/(m_0^2 \omega^2) P^2$ and V_2 and V_1 are the volumes of the nanoparticle with and without shell, respectively. Unlike charge transfer to a defect state, the energy transfer model is intrinsically weakly temperature-sensitive, inasmuch as the overtone absorptions of the ligands do not depend on temperature.

Neglecting local field and orientational effects, the absorption cross section of the shell σ_{shell} is related to the ligand molar absorption coefficient ϵ_{ligand} as

$$\sigma_{\text{shell}} = 4\pi R^2 C_K \frac{\ln 10}{N_A} \epsilon_{\text{ligand}} \quad (3)$$

where N_A is the Avogadro constant and C_K is the ligand number per unit surface area on the PbSe nanocrystal. σ_{shell} can also be expressed as a function of the imaginary dielectric constant ϵ'' (CGS, see the Supporting Information)

$$\sigma_{\text{shell}} = 18\pi \epsilon'' \frac{V_2}{\lambda} \frac{1-f}{1+2f\sqrt{\epsilon_m}(\epsilon_1+2\epsilon_m)^2} \quad (4)$$

where $f = V_1/V_2$ represents the ratio of nanocrystal's volume to total volume. Equations 3 and 4 lead to an expression of ϵ'' .

We assume that the ligand surface number density C_K is the same for all samples, and we substitute the particle size radius, R , by the emitting photon energy $\hbar\omega$ according to the linear fitting $\hbar\omega = A/R^2 + B$. On the basis of the TEM size determination of the samples in the size range studied, A is 3.2 eV·nm² and B is 0.41 eV. The nonradiative rate is then calculated as (in CGS units)

$$T_{\text{nr}}^{-1} = \frac{12}{64} \times \frac{16\pi^2 A C_K}{81\hbar\omega^3(\hbar\omega - B)} \frac{e^2 c P^2}{m_0^2} \left(\frac{3\varepsilon_m}{\varepsilon_1 + 2\varepsilon_m} \right)^2 \times \frac{\sqrt{\varepsilon_m(\varepsilon_1 + 2\varepsilon_m)^2 V_1^{-1} - V_2^{-1} V_2 + 2V_1 \ln 10}}{2\varepsilon_m^2 + \varepsilon_1^2} \frac{V_2 - V_1}{V_2} \frac{2V_1 \ln 10}{N_A} \varepsilon_{\text{ligand}} \quad (5)$$

where 12/64 is the degeneracy factor.

We used $C_K = n_{\text{ligand}}/(4\pi R^2 n_{\text{PbSe}}) = 5.7 \text{ nm}^{-2}$, which is calculated based on the absorption peak height of CH stretch and PbSe exciton. (See the Supporting Information.) For TCE, $\varepsilon_m = 2.25$, for PbSe, $\varepsilon_1 = 23$, and the molecular length for the ligand (lead oleate) $\Delta R = 1.8 \text{ nm}$. As shown in Figure 2, eq 5 and the simple dipole coupling model explain rather well the general trends but also some of the details. The model captures well the nonmonotonic order of magnitude drop in PL lifetimes arising from the overtone bands. In Figure 2, the small decrease from 0.8 to 0.9 eV of the predicted PLQY (from 100 to 80%) arises from the very weak third overtone in the CH absorption spectrum, whereas the 100% PLQY reflects that the absorption of the ligands is below the spectrometer sensitivity. Such small variation is beyond the accuracy of the measurement. While this paper was under review, a similar work¹⁵ was published that reports the absolute quantum yield of PbSe nanocrystal, and it also shows that dipolar energy transfer to the ligand vibrations accounts rather well for the observed trends.

As shown in Figure 3, the effect of ligands is also reflected by the fact that replacing the ligands can change the decay lifetime. Ligand replacement is difficult with PbSe but standard with CdSe. For this purpose, a PbSe nanocrystal with a PL wavelength of $2.07 \mu\text{m}$ (0.60 eV) was treated for 20 min with CdOA. This shifts the PL to $1.89 \mu\text{m}$ wavelength (0.66 eV), with the lifetime increasing from 345 (± 9 ns) to 416 ns (± 16 ns). The oleate ligands are then replaced with perfluorotetradecanoic acid and the PbSe/CdSe nanocrystals dissolved in perfluoro-1,3-dimethylcyclohexane solvent; the sample's PL energy stayed the same, whereas the lifetime increased by another $\sim 50\%$. The trend is correct, but on the basis of absorbance of the neat fluorinated ligands, the expected lifetimes should be much longer than we observed. As of now, we have not been successful in obtaining a clean IR spectra of the solution after transfer in the perfluorosolvent so that it is very likely that the ligand exchange is only partial.

It is predicted that the radiative lifetime increases by three orders of magnitude when the sample is cooled from room temperature to a few kelvin,¹¹ but such a large effect has not been observed experimentally.¹³ As shown in Figure 4, as the sample is cooled from room temperature to 14 K, the PL energy decreases from 0.72 to 0.65 eV owing to the reduction of the band gap, whereas the PL intensity does not change significantly. From the model above and Figure 2, energy transfer to the ligand vibration will not increase significantly because of this shift, and it should be mostly temperature-independent. The similar brightness therefore confirms that energy transfer to surface traps is unlikely to be a significant contribution to the nonradiative decay. However, the lifetime increased from 200 ns to nearly 1 μs , as shown in Figure 5. We can attempt to account for this result considering that out of the nearly degenerate first excitons in PbSe, there are bright states and dark states at a slightly lower energy.¹¹ Dark states should have much longer lifetime such that decay to the ground state requires thermal activation into the bright states. In this simplistic picture of perfectly degenerate dark states of degeneracy 52 and bright states of degeneracy 12 at a higher energy Δ with no mixing, the temperature

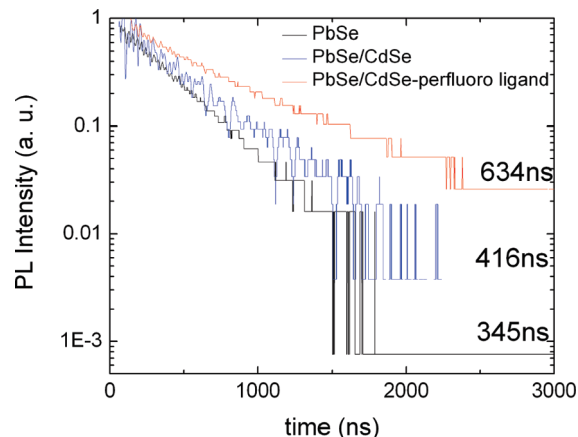


Figure 3. PL decay traces for one set of samples with different surface treatment. The black line is for the starting PbSe nanocrystal. The blue and red lines are for PbSe with a CdSe shell. Blue is with oleate ligand and red is after ligand exchange with perfluorotetradecanoate ligands.

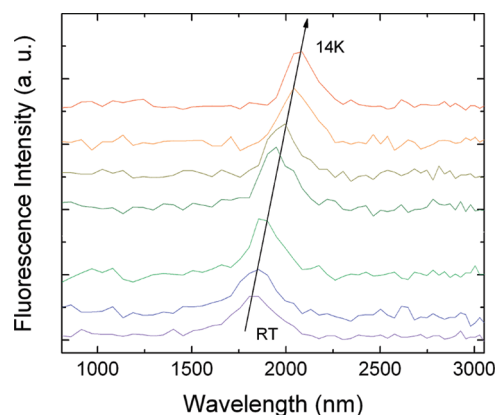


Figure 4. PL energy shift as a function of temperature for PbSe nanocrystals of 0.72 eV room temperature PL. The integrated intensity changes by less than $\sim 25\%$.

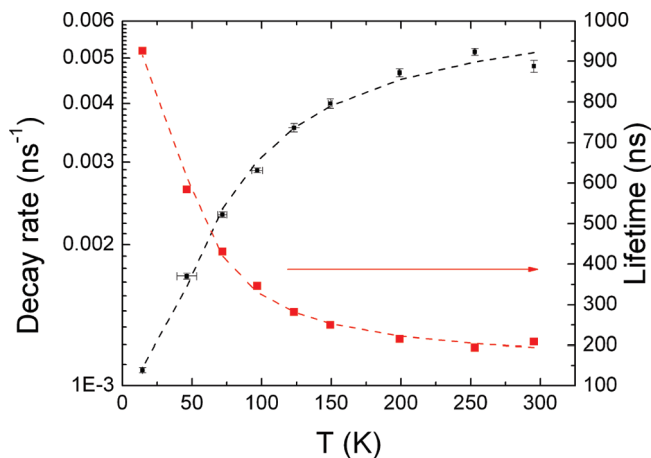


Figure 5. PL lifetime and the corresponding decay rates as a function of temperature for PbSe nanocrystals of 0.72 eV room-temperature exciton. The dashed lines are fits using eq 6.

dependence of the total lifetime can be well fitted to a phenomenological expression

$$T^{-1} = \frac{52t_d^{-1} + 12t_b^{-1} \exp(-\Delta/k_B T)}{52 + 12 \exp(-\Delta/k_B T)} \quad (6)$$

where τ_b^{-1} and τ_d^{-1} are the bright and dark state decay rates, respectively. The curve fitting parameter gives $\Delta = 10 \pm 1$ meV, broadly consistent with the values calculated in ref 11. The bright-state decay rate $\tau_b^{-1} = 0.031 \pm 0.002$ ns⁻¹ and the dark state rate $\tau_d^{-1} = 0.0011 \pm 0.0002$ ns⁻¹. The nonradiative mechanism of dipole energy transfer to the ligand vibrations is temperature-independent, but it depends directly on the radiative decay rates. This is why such a temperature-independent nonradiative mechanism with bright and dark states can lead to similar brightness but different lifetimes as a function of temperature.

IV. Conclusions

In conclusion, we measured the infrared PL lifetime of PbSe colloidal QDs. The larger PbSe nanocrystals exhibit shorter lifetimes in a trend opposite to the expected trend for radiative decay. A dipole model of energy transfer to ligands vibrations accounts fairly well for the nonradiative energy relaxation of PbSe at room temperature. This confirms that ligands vibration is one of the main obstacles to high efficiency infrared radiation from colloidal QDs. At low temperature, PbSe showed a longer PL lifetime but less than expected because of the role of nonradiative decay.

Acknowledgment. We acknowledge Dr. Anshu Pandey for help on synthesis and experimental setup. The research was supported by the U.S. National Science Foundation NSF under grant no. DMR-0706268. We made use of shared facilities supported by the NSF MRSEC program under DMR-0820054.

Supporting Information Available: Derivation of dipolar energy transfer model; absorption spectra of lead oleate ligands;

and size-energy dependence of the PbSe nanocrystals. This material is available free of charge via the Internet at <http://pubs.acs.org>.

References and Notes

- (1) Wehrenberg, B. L.; Wang, C.; Guyot-Sionnest, P. *J. Phys. Chem. B* **2002**, *106*, 10634–10640.
- (2) Du, H.; Chen, C.; Krishnan, R.; Krauss, T. D.; Harbold, J. M.; Wise, F. W.; Thomas, M. G.; Silcox, J. *Nano Lett.* **2002**, *2*, 1321–1324.
- (3) Pietryga, J. M.; Schaller, R. D.; Werder, D.; Stewart, M. H.; Klimov, V. I.; Hollingsworth, J. A. *J. Am. Chem. Soc.* **2004**, *126*, 11752–11753.
- (4) Guyot-Sionnest, P.; Wehrenberg, B.; Yu, D. *J. Chem. Phys.* **2005**, *123*, 074709.
- (5) Talapin, D. V.; Murray, C. B. *Science* **2005**, *310*, 86–89.
- (6) Pietryga, J. M.; Werder, D. J.; Williams, D. J.; Casson, J. L.; Schaller, R. D.; Klimov, V. I.; Hollingsworth, J. A. *J. Am. Chem. Soc.* **2008**, *130*, 4879–4885.
- (7) Moreels, I.; Lambert, K.; De Muynck, D.; Vanhaecke, F.; Poelman, D.; Martins, J. C.; Allan, G.; Hens, Z. *Chem. Mater.* **2007**, *19*, 6101–6106.
- (8) Moreels, I.; Lambert, K.; Smeets, D.; De Muynck, D.; Nollet, T.; Martins, J. C.; Vanhaecke, F.; Vantomme, A.; Delerue, C.; Allan, G.; Hens, Z. *ACS Nano* **2009**, *3*, 3023–3030.
- (9) Moreels, I.; Allan, G.; De Geyter, B.; Wirtz, L.; Delerue, C.; Hens, Z. *Phys. Rev. B* **2010**, *81*, 235319.
- (10) Kang, I.; Wise, F. W. *J. Opt. Soc. Am. B* **1997**, *14*, 1632–1646.
- (11) An, J. M.; Franceschetti, A.; Zunger, A. *Nano Lett.* **2007**, *7*, 2129–2135.
- (12) An, J. M.; Franceschetti, A.; Dudiy, S. V.; Zunger, A. *Nano Lett.* **2006**, *6*, 2728–2735.
- (13) Kigel, A.; Brumer, M.; Maikov, G.; Sashchiuk, A.; Lifshitz, E. *Superlattices Microstruct.* **2009**, *46*, 272–276.
- (14) Aharoni, A.; Oron, D.; Banin, U.; Rabani, E.; Jortner, J. *Phys. Rev. Lett.* **2008**, *100*, 057404.
- (15) Semonin, O. E.; Johnson, J. C.; Luther, J. M.; Midgett, A. G.; Nozik, A. J.; Beard, M. C. *J. Phys. Chem. Lett.* **2010**, *1*, 2445–2450.

JP105818E